 E-ISSN: 2303-0720

DOI: https://doi.org/10.21009/JRSKT.112.02

Synthesis of Nd-Pheophytin Complex and Its Hydrolysis into Nd-Pheophorbide from Katuk Leaves (*Sauropus androgynous* (L.) Merr)

Fadia Novayanti, Adhitiyawarman*, Winda Rahmalia

Universitas Tanjungpura, Jl. Prof. Dr. Hadari Nawawi, Kec. Bansir Laut, Pontianak City, West Borneo 78124, Indonesia

*Email: adhitiyawarman@chemistry.untan.ac.id

Received: 24 September 2025
Revised: 20 November 2025
Accepted: 24 November 2025
Online: 15 December 2025
Published: 30 December 2025

Jurnal Riset Sains dan Kimia Terapan
p-ISSN: 2302 - 8467
e-ISSN: 2303 – 0720

Abstract

Pheophorbide, as a chlorophyll derivative, has potential as a complexing ligand for heavy metals, including lanthanides. The synthesis of Nd-pheophytin complex and its more polar Nd-pheophorbide (pheophytin's hydrolyzed product) were investigated using pheophytin isolated from Katuk's (*Sauropus androgynus* L. Merr.) leaves. This study aims to determine the optimal reaction conditions and the complex characteristics. Pheophytin ligand and Nd were complexed under two different reaction conditions: room temperature and reflux at 65 °C for 10 hours. The pheophytin starting material was obtained by preparative thin-layer chromatography (PTLC), yielding 0.02 g. UV-vis analysis revealed characteristic absorption bands at 404 nm (Soret band) and 666 nm (Q band) in methanol, while FTIR spectra confirmed the presence of functional groups corresponding to pheophytin. The Nd-pheophytin complex formation was indicated by hypsochromic shifts in UV-vis spectra, suggesting the Nd^{3+} complexing. Fluorescence spectra between pheophytin and Nd-pheophytin showed distinct emission patterns, with pheophytin exhibiting peaks at 662 and 722 nm, while Nd-pheophytin displayed peaks with shoulders at 654 and 714 nm. Hydrolysis of Nd-pheophytin using 1 M NaOH at pH 10 produced Nd-pheophorbide. TLC analysis showed a decrease in the Rf value of Nd-pheophytin to Nd-pheophorbide from 0.95 to 0.43, with tailing, attributed to the higher polarity of pheophorbide. These findings confirm the successful synthesis and hydrolysis of the Nd-pheophytin complex.

Keywords: lanthanide, neodimium, pheophytin complex, pheophorbide complex, synthesis.

 E-ISSN: 2303-0720

Introduction

Katuk leaves (*Sauropus androgynus* (L.) Merr.) belong to the family Euphorbiaceae, order Euphorbiales. The dark green coloration of Katuk leaves indicates a high chlorophyll content, which is beneficial for skin rejuvenation and supports the circulatory system (Majid & Muchtaridi, 2018). Several studies have confirmed Katuk leaves' relatively high chlorophyll content. Nurdin et al. (2009) reported a chlorophyll concentration of 1509.1 mg/kg, while Utami & Anjani (2016) reported chlorophyll A at 1136.6 mg/kg and chlorophyll B at 372.5 mg/kg. Katuk leaves have been identified as potential photosensitizing agents, fulfilling essential criteria such as selectivity, efficiency, chemical stability, broad absorption wavelength spectrum, solubility, and non-toxicity. Furthermore, Riansyah et al. (2021) reported that Katuk leaves exhibit greater stability than those of Suji, Pandan, and Moringa.

Chlorophyll is a natural pigment that plays a vital role in plant photosynthesis, functioning as a light harvester, energy transfer agent, and converter of light energy, with an absorption range of 400-700 nm. Chlorophyll has been widely applied in various fields, including as a natural coloring agent, in pharmaceuticals, as a bioinsecticide, as a photosensitizer in cancer therapy, and in dye-sensitized solar cells (Pratiwi et al., 2015). Structurally, chlorophyll consists of a porphyrin ring coordinated with Mg^{2+}. This coordination bond is relatively unstable, making chlorophyll susceptible to degradation. Enzymatic activity and environmental factors can also accelerate chlorophyll degradation. Pheophorbide, the defitilated and demetalated derivative of chlorophyll, retains a porphyrin structure with four nitrogen atoms, each possessing lone pairs that function as electron-donor ligands in metal complex formation (Saide et al., 2020).

The use of chlorophyll derivatives as ligands capable of forming complexes with rare-earth metals has attracted significant scientific interest. Erzunov et al. (2022) reported that the porphyrin ring in chlorophyll can form stable lanthanide–porphyrin complexes. Tao et al. (2001) successfully synthesized pheophytin complexes with lanthanide metals, confirming that lanthanum (La) coordinates with the porphyrin ring. Similarly, Choi (2019) reported that the lanthanides gadolinium (Gd) and lutetium (Lu) can coordinate to the porphyrin ring of pheophorbide, resulting in absorption bands between 700 and 800 nm.

Research on porphyrins and their derivatives has advanced rapidly, particularly in their potential applications in biomedicine, photocatalysis, optical sensors, and photodynamic therapy (PDT). Among these, the formation of complexes between porphyrins and lanthanides, such as neodymium (Nd^{3+}), has garnered special attention. The Nd^{3+} ion has a unique electronic configuration and emits luminescence in the near-infrared region, enabling deeper tissue penetration than visible light and making it advantageous for medical applications.

Nd–pheophytin was synthesized, and the resulting complexes demonstrate notable stability and photophysical activity, making them promising candidates for both cancer diagnosis and therapy. In this study, the Nd-pheophytin complex was hydrolyzed to yield Nd, a reaction not previously reported. This hydrolysis was intended to produce a more polar, water-soluble compound, thereby enhancing its suitability for biomedical applications that require high solubility and efficient biological distribution, particularly as a photosensitizer in PDT. Consequently, this study focuses on the modification of Nd–pheophytin complexes into Nd–pheophorbide to investigate the complexation behavior of lanthanides with chlorophyll-derived ligands. Reaction conditions, namely room temperature and reflux during the complex formation, were investigated. The structural and photophysical properties of the synthesized complexes were analyzed by UV-vis spectroscopy and fluorescence spectroscopy.

Method

Material and Equipment

The substances used in this investigation are $NdCl_3.6H_2O$ (Sigma Aldrich), Katuk leaves (*Sauropus androgynus* (L.) Merr.), Preparative TLC Plate (Sigma Aldrich), Distilled water (H_2O), hydrochloric acid (Merck), acetone (Sigma Aldrich), ethyl acetate (Sigma Aldrich), methanol (Merck), sodium hydroxide (Merck), petroleum ether (Smart-Lab), and cyclohexane (Merck).

 E-ISSN: 2303-0720

The equipment utilized in this study are vial bottles, graduated pipettes, analytical balance, separation funnel, Erlenmeyer flasks, a reflux apparatus, thermometer, chromatography chamber, beakers, hot plate, filter paper, thin-layer chromatography (TLC) equipment, micropipette, magnetic stirrer, capillary tubes, Fourier Transform Infrared (FTIR) spectrophotometer, UV-vis spectrophotometer and fluorescence spectrometer (Horiba FluoroMax Hybrid).

Preparation and Extraction of Katuk Leaves

Katuk leaves were separated from their stems, and any yellowish-brown leaves were discarded. The fresh green leaves were thoroughly washed with running water to remove impurities, then placed on trays to dry in direct sunlight. Once dried, the leaves were cut into small pieces and weighed (Syahadat et al., 2020).

Extraction of katuk leaves was carried out with modifications based on the methods of Pesang et al. (2020) and Kusmita et al. (2015). The powdered leaf sample was placed into a container, and acetone was added until the sample was fully submerged. The mixture was macerated for 1 hour with occasional stirring, while the container was covered with aluminum foil to prevent light exposure. The extract was filtered using filter paper and air-dried at room temperature to obtain a concentrated Katuk leaf extract. The extract was then characterized using UV-Vis spectrophotometry and thin-layer chromatography (TLC), employing a mobile phase consisting of petroleum ether: cyclohexane: ethyl acetate: acetone: methanol (6:1.6:1:1:0.4, v/v) (Quach et al., 2004).

Isolation and Identification of Pheophytin

Pheophytin was isolated using preparative thin-layer chromatography (PTLC). A total of 25 mg of Katuk leaf extract was dissolved in 2 mL of acetone and thoroughly mixed. The sample was then spotted onto a glass plate coated with silica gel and eluted using the mobile phase petroleum ether: cyclohexane: ethyl acetate: acetone: methanol (6:1.6:1:1:0.4, v/v). The target compound was collected by scraping the corresponding band, dissolving it in acetone, filtering, and then drying the solution. The isolated compound was further analyzed by TLC, FTIR, and UV-Vis spectrophotometry by dissolving the complex in methanol, then measuring its absorbance between 300 and 800 nm (Notonegoro et al., 2022).

Synthesis of Nd–Pheophytin Complex

The Nd–pheophytin complex was synthesized by reacting pheophytin with $NdCl_3 \cdot 6H_2O$ in a 2:1 molar ratio. Pheophytin (0.0011 g) was dissolved in methanol with continuous stirring until homogeneous. $NdCl_3 \cdot 6H_2O$ (0.0002 g) was separately dissolved in methanol, and the solution was slowly added to the pheophytin solution with stirring. The total volume was adjusted to 10 mL using methanol. Complexation reactions were conducted under two conditions: (i) at room temperature for 24 hours (Method 1) and (ii) under reflux for 10 hours (Method 2). TLC analyzed the resulting complexes; UV-vis spectrophotometry by dissolving the complex in methanol, then measuring its absorbance between 300 and 800 nm; and fluorescence spectroscopy by dissolving the complex in methanol, then measuring its emission between 450 and 900 nm with an excitation wavelength of 404 nm (Anjelia et al., 2019).

Hydrolysis of Nd–Pheophytin to Nd–Pheophorbide

The synthesized Nd–pheophytin complex was subjected to hydrolysis to remove the phytol group. Hydrolysis was performed by adding 0.1 M NaOH as a strong base until the pH reached 10, followed by refluxing for 30 minutes. The mixture was then filtered, neutralized with 0.1 M HCl, and analyzed using TLC (Adhitiyawarman & Lowe, 2018).

 E-ISSN: 2303-0720

Result and Discussion

Preparation and Extraction of Katuk Leaves

The chlorophyll source used in this study was obtained from Katuk leaves collected in Batu Layang, North Pontianak District. Katuk leaves contain a relatively high and more stable chlorophyll content compared to other leaves such as Suji, pandan, and moringa. The cleaned Katuk leaves were dried under direct sunlight. A total of 200 g of fresh Katuk leaves were subjected to sun-dried.

Drying was conducted to reduce the moisture content of the leaves and simultaneously facilitate chlorophyll degradation into pheophytin (Adhamatika & Murtini, 2021). Resita et al. (2010) reported that dried leaves contain higher levels of pheophytin compared to fresh leaves. This occurs because, during the drying process, the magnesium atom in the porphyrin ring of chlorophyll is replaced by two hydrogen atoms, forming pheophytin. Consequently, more pheophytin is generated in dried leaves (Wihenti et al., 2021). The dried Katuk leaves weighed 44.5 g and were subsequently extracted by maceration with acetone.

Extraction was performed by maceration to preserve heat-sensitive compounds (Pasaribu et al., 2025). Acetone, a semipolar solvent, can extract both polar and nonpolar compounds, making it suitable for Katuk leaf extraction (Sekali et al., 2020; Sumiati, 2021). The maceration was performed for 1 hour with continuous stirring to accelerate the process. The reaction was carried out in the dark to prevent light-induced degradation.

The concentrated Katuk leaf extract obtained was 0.11 g and appeared as a dark green residue. The extract was then identified by thin-layer chromatography (TLC) using a mobile phase of petroleum ether: cyclohexane: ethyl acetate: acetone: methanol (6:1.6:1:1:0.4, v/v) and a silica gel stationary phase (Quach et al., 2004). The separated compounds appeared as distinct spots on the TLC plate. Separation occurred due to differences in the solubility of the compounds in the mobile phase, resulting in different Rf values (Suria et al., 2024). TLC characterization was performed to determine the number and types of pigments present in the Katuk leaf extract. TLC analysis of the acetone extract revealed six spots, with colors identified as orange-yellow, gray, yellow-green, blue-green, yellow, and pale gray. Based on Rf values, these were identified as β-carotene, pheophytin, chlorophyll a, chlorophyll b, xanthophyll, and pheophorbide. Pheophytin appeared as a dark gray spot with an Rf value of 0.8. Due to its nonpolar nature, pheophytin migrated with the nonpolar mobile phase. The TLC results and Rf values of the Katuk leaf extract are presented in **Figure 1** and **Table 1.**

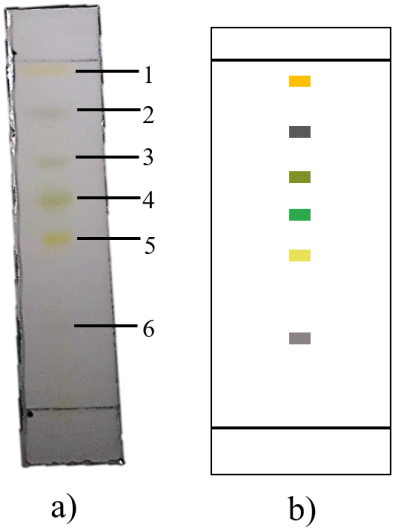

Figure 1. TLC results of katuk leaf acetone extract (a) and schematic illustration (b)

 E-ISSN: 2303-0720

Table 1. Rf values of chlorophyll extract.

No.	Rf Sample	Colour	Compound	Rf References
1	0,91	Yellowish orange	*β*-carotene	0,95
2	0,72	Gray	Pheophytin a	0,7-0.8
3	0,67	Greenish yellow	Chlorophyll a	0,44[a]
4	0,55	Bluish green	Chlorophyll b	0,32[a]
5	0,44	Yellow	Xanthophyll	0,46[b]
6	0,22	Light gray	Pheophorbide	0,16-0,20

The Katuk leaf extract was further analyzed using the UV-Vis spectrophotometric method within the wavelength range of 350–800 nm (**Figure 2**). Chlorophyll absorbs light in two wavelength ranges, 400–450 nm and 500–700 nm, which are identified as the Soret/B band and the Q band, respectively. This absorption arises from $\pi \rightarrow \pi^*$ electronic transitions within the porphyrin ring (Anjelia et al., 2019; Wahyuni & Setiarso, 2022). The Soret band exhibits strong absorption intensity, while the Q band shows relatively weak absorption (Saleh & Halidun, 2022).

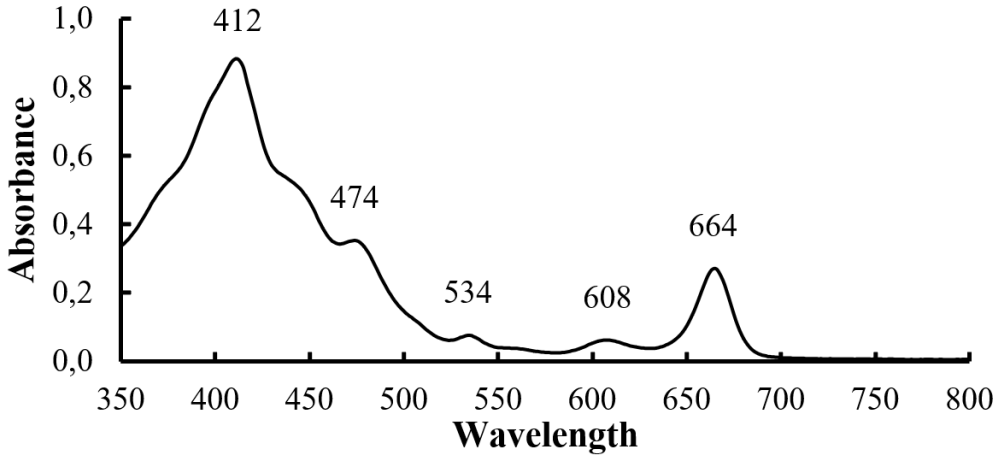

Figure 2. Absorbance spectrum of katuk leaf extract

Based on **Figure 2**, the Katuk leaf extract shows major absorption peaks at 412 and 662 nm, accompanied by weaker peaks at 534 and 608 nm, which are characteristic of chlorophyll compounds. The peak at 412 nm in the Soret band region corresponds to the absorption of chlorophyll a and b. Peaks at 534, 608, and 664 nm in the Q band region indicate the porphyrin orbital structure consisting of four pyrrole rings. Meanwhile, the peak at 474 nm corresponds to carotenoid absorption. A similar absorption pattern was reported by Yusprianto et al. (2021) and Anjelia et al. (2019)

Isolation and Identification of Pheophytin

The identification results of *Sauropus androgynus* (Katuk) leaf extract indicated the presence of several components; therefore, further purification was necessary to obtain pure pheophytin. Pheophytin isolation was carried out using preparative thin-layer chromatography (PTLC). The PTLC isolation process is based on differences in adsorption capacity, partition behavior, and solubility of each chemical component, which are determined by the polarity of the mobile phase. Since the adsorbent interacts differently with each component, their migration rates vary, leading to separation (Pratiwi et al., 2015).

The separation was performed on a 20 × 20 cm glass plate using the five-solvent eluent system, resulting in six colored bands on the PTLC plate (**Figure 3**). The banding pattern showed colors and positions similar to those observed in TLC of the crude extract. The separation was satisfactory, with each band well resolved and not overlapping, making scraping feasible. The gray band corresponding to pheophytin was carefully scraped off, dissolved in acetone, and filtered. The filtrate was subsequently re-analyzed using TLC.

 E-ISSN: 2303-0720

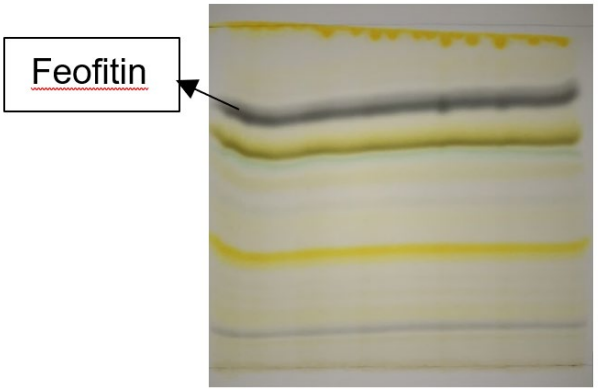

Figure 3. PTLC result of Katuk leaf extract using a five-solvent eluent system (petroleum ether: cyclohexane: ethyl acetate: acetone: methanol, 6:1.6:1:1:0.4).

Figure 4. TLC result of isolated pheophytin.

The TLC test (**Figure 4**) showed a dominant gray spot with an Rf of 0.63, identified as pheophytin. This indicates that the isolated pheophytin was free from β-carotene and other chlorophyll derivatives. The amount of pheophytin obtained from PTLC separation was 0.02 g.

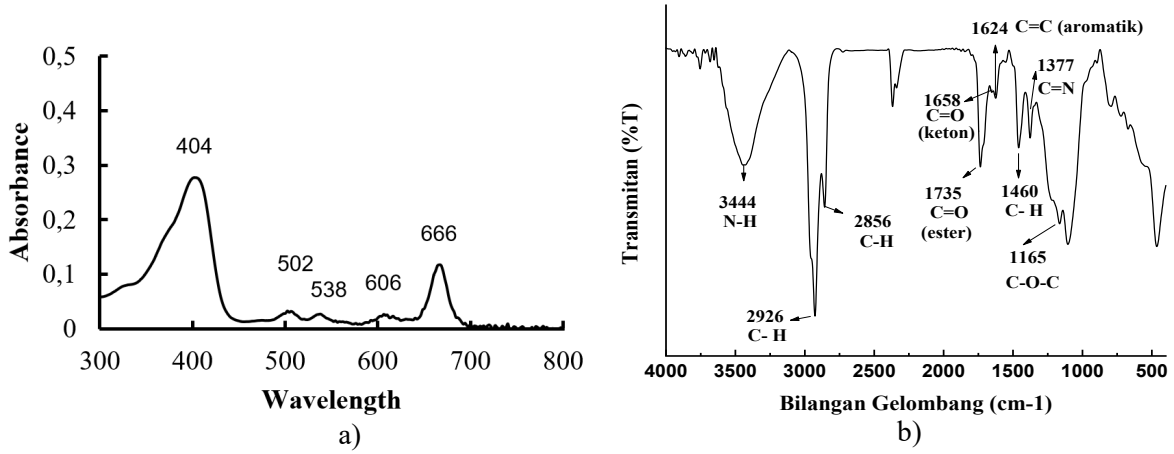

Figure 5. a) UV-vis spectrum of pheophytin in methanol and b) FTIR spectrum of isolated pheophytin.

The UV–vis spectrum of pheophytin exhibited major absorption peaks at 404 nm and 666 nm, along with minor absorption peaks at 502, 538, and 606 nm (**Figure 5a**). This absorption pattern is characteristic of pheophytin and is consistent with previous reports (Kusmita et al., 2015). The main absorption peak in the Soret band region showed an 8 nm blue shift compared to the extract of Katuk leaves, while the Q band exhibited a 2 nm red shift.

 E-ISSN: 2303-0720

The FTIR characterization of isolated pheophytin (**Figure 5b**) showed characteristic absorption peaks consistent with previous reports (Mohammed et al., 2019). The absorption band at 3435 cm^{-1} corresponds to the N–H group, indicating the loss of Mg^{2+} and its replacement with two protons (H^+). The presence of the phytol chain was confirmed by C–H stretching at 2925 cm^{-1}, while the absorption at 2859 cm^{-1} corresponds to methylene (–CH_2–) groups. The band at 1732 cm^{-1} represents ester C=O stretching, while the 1626 cm^{-1} band indicates ketone C=O stretching. Absorptions at 1456 cm^{-1} and 1375 cm^{-1} were attributed to aromatic C=C and C=N groups, respectively. Furthermore, the band at 1164 cm^{-1} corresponds to C–O–C bridge vibrations (Nandiyanto et al., 2019).

Synthesis of Nd–Pheophytin Complex

The Nd–pheophytin complex was synthesized by reacting isolated pheophytin with $NdCl_3 \cdot 6H_2O$. The $NdCl_3 \cdot 6H_2O$ solution served as a source of Nd^{3+} ions, acting as the central metal, while pheophytin functioned as the electron-donor ligand. The complexation reaction was carried out in methanol using two methods (**Figure 6**).

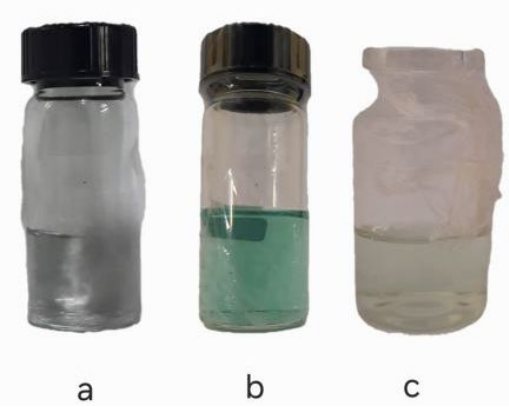

Figure 6. Photographs of pheophytin solution (a), Nd–pheophytin at room temperature (b), and Nd–pheophytin under reflux (c).

In method 1, the solution color changed from pale gray to deep bluish-green (**Figure 6b**). In contrast, method 2 produced a yellowish-green solution (**Figure 6c**), likely due to pheophytin degradation at elevated temperatures. These color changes indicate the formation of Nd–pheophytin. The literature reports confirm that metalloporphyrin formation, achieved by replacing Mg^{2+} with a higher-affinity ion, restores the green color characteristic of chlorophyll derivatives (Usman et al., 2022).

TLC analysis was performed by comparing the pheophytin sample with Nd-pheophytin at room temperature and at reflux, as observed under UV light. Based on TLC observations, two spots were observed in the complexation reaction using method 1 (**Figure 7a**). The TLC results of the Nd-pheophytin method 1 showed two faint spots (**Figure 7b**). The first spot was at the same position as pure pheophytin; the second spot had a much lower Rf but was less visible. Meanwhile, in the TLC results for method 2 (Nd-pheophytin), two spots showed greater intensity than at room temperature (**Figure 7c**). The first spot was at the same Rf as pure pheophytin; the second spot was faintly below pheophytin. The presence of pheophytin spots indicates that there was still pheophytin that had not reacted with Nd^{3+} ions.

The absorption spectra of pheophytin and Nd–pheophytin complexes (room temperature and reflux conditions) in methanol are presented in **Figure 8**. Pheophytin exhibited absorption peaks at 404 nm (Soret band) and 666 nm (Q band). The Nd–pheophytin complex prepared by method 1 showed a bathochromic shift in the Soret band from 404 to 408 nm, while the Q band shifted from 666 to 664 nm. In contrast, the complex obtained by method 2 exhibited a hypsochromic shift in the Soret band from 404 to 400 nm. A hypsochromic shift, or shift toward shorter wavelengths, occurs due to charge transfer between the metal and ligand during coordination bond formation. The relatively small shift suggests an incomplete reaction between Nd^{3+} ions and pheophytin. The Q band also shifted hypsochromically from 666 to 664 nm, indicating interactions between the Nd^{3+} valence electrons and

 E-ISSN: 2303-0720

the π-electron system (Orzeł et al., 2017). The hypsochromic shifts observed in both the Soret and Q bands confirm the successful formation of the Nd–pheophytin complex, consistent with previous reports (Kang et al., 2018). Similar hypsochromic shifts have been reported for the metallation of pheophytin with other metals. Das et al. (2022) reported that Fe–pheophytin exhibited Soret and Q band shifts from 410 and 660 nm to 395 and 620 nm, respectively, while Sandiningtyas & Suendo (2010) observed shifts from 405 and 669 nm to 393 and 626 nm.

Figure 7. TLC analysis of pheophytin (a), Nd–pheophytin (method 1) (b), and Nd–pheophytin (method 2) (c).

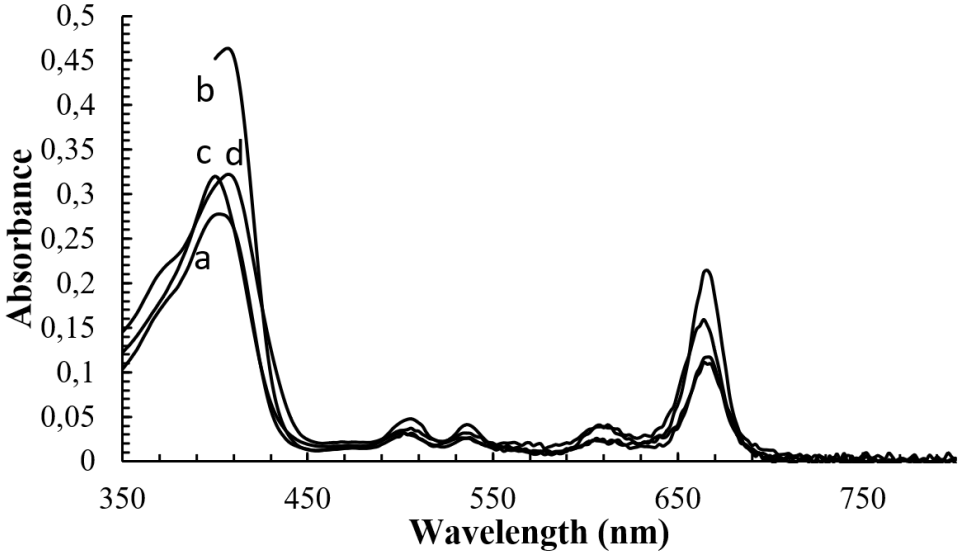

Figure 8. UV–vis absorption spectra of pheophytin (a), Nd–pheophytin (overall) (b), Nd–pheophytin under reflux for 10 h (c), and Nd–pheophytin at room temperature for 24 h (d).

 E-ISSN: 2303-0720

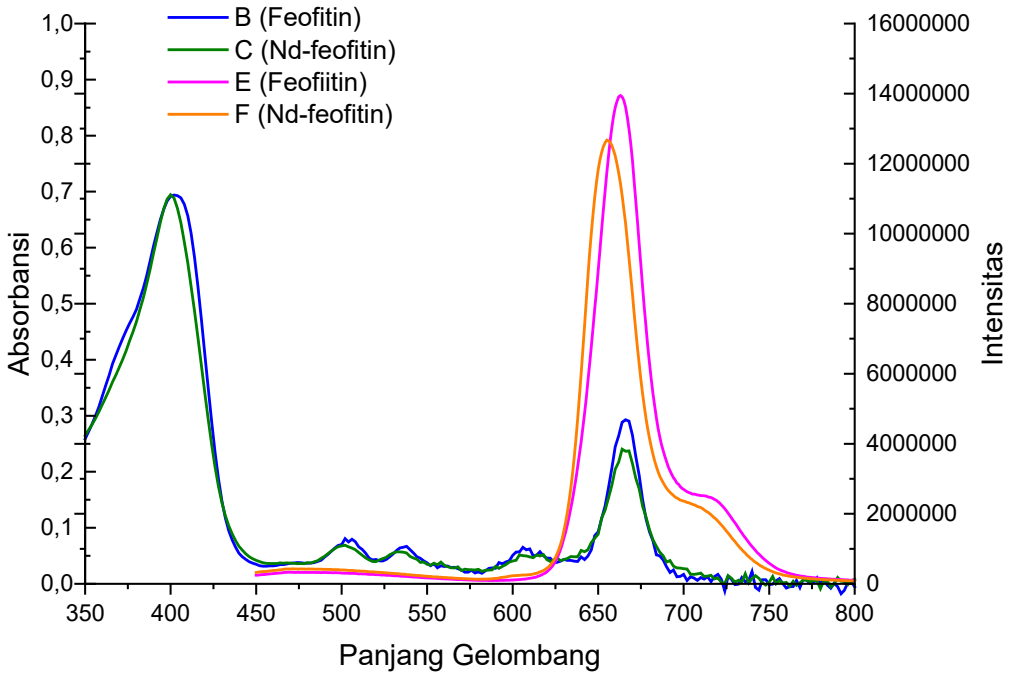

Figure 91. Normalized absorption and emission spectra of pheophytin and Nd–pheophytin.

The emission spectrum of the Nd-pheophytin complex was observed within the wavelength range of 450–800 nm (**Figure 9**). This selection was based on the UV–vis analysis, which showed that the Nd–pheophytin complex synthesized by method 2 yielded results consistent with the literature. The emission of Nd–pheophytin was then compared with that of isolated phycocyanin. The spectra showed that Nd–pheophytin exhibited emission peaks with shoulders at 654 and 714 nm, while pheophytin displayed peaks at 662 and 722 nm. These pheophytin peaks are consistent with the report by Lopes & Courrol (2023). Furthermore, the emission intensity of Nd–pheophytin was found to be lower than that of pheophytin. This decrease in intensity is assumed to occur because part of the absorbed energy in Nd–pheophytin is transferred to the central Nd^{3+} ion (Syahputri et al., 2024). This behavior is common in porphyrin–lanthanide metal systems, where Nd^{3+} ions possess energy levels capable of accepting energy transfer from the ligand. In addition, the normalized absorption spectra presented in the figure reveal a hypsochromic (blue) shift in the Soret band region, accompanied by a decrease in intensity in the Q band region, which also appears slightly broader. This phenomenon is likely due to interactions between the central Nd^{3+} ion and the pheophytin ligand. The structure of the Nd–pheophytin complex can be seen in **Figure 10** as follows:

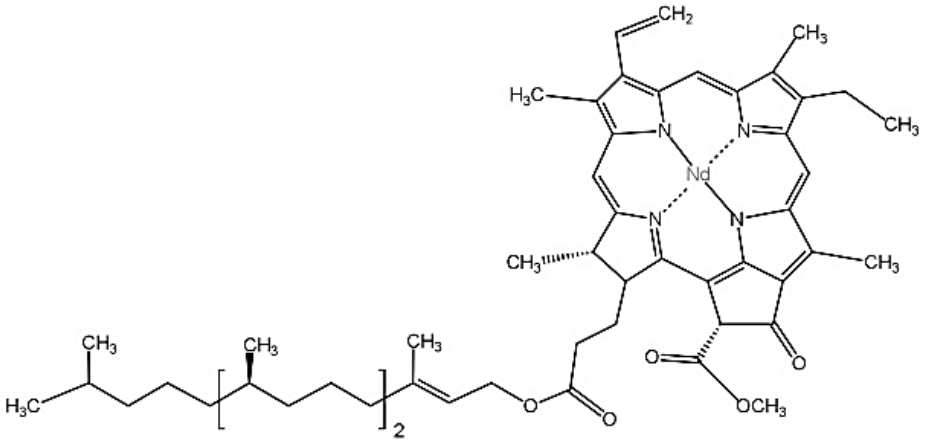

Figure 10. Structure of the Nd–pheophytin complex

 E-ISSN: 2303-0720

Hydrolysis of Nd-pheophytin into Nd-pheophorbide

The phytol group in the Nd-pheophytin complex was subsequently hydrolyzed using 0.1 M NaOH. Defitilization of the phytol group in the porphyrin structure can occur via an enzymatic or chemical pathway, namely acid–base hydrolysis. The hydrolysis product was then analyzed by TLC, as shown in **Figure 11**.

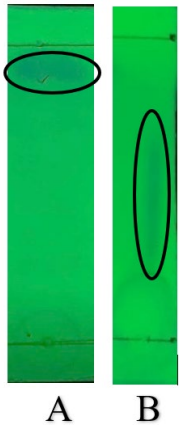

Figure 21. TLC results: (a) Nd-pheophytin complex and (b) Nd-pheophorbide complex after hydrolysis

Based on **Figure 11**, the TLC observation after the hydrolysis reaction showed a decrease in the Rf value with tailing, from 0.90 to 0.43. This indicates the removal of the phytol group, yielding Nd-pheophorbide with higher polarity. Tailing may occur due to interactions between the silica stationary phase's polar silanol groups and the polar compounds in the sample. Because pheophorbide ligands are polar, the Nd-pheophorbide complex was eluted more slowly, tending to be retained on the stationary phase, and thus formed tailing. The hydrolysis reaction of the phytol group in the Nd-pheophytin complex is illustrated in **Figure 12**.

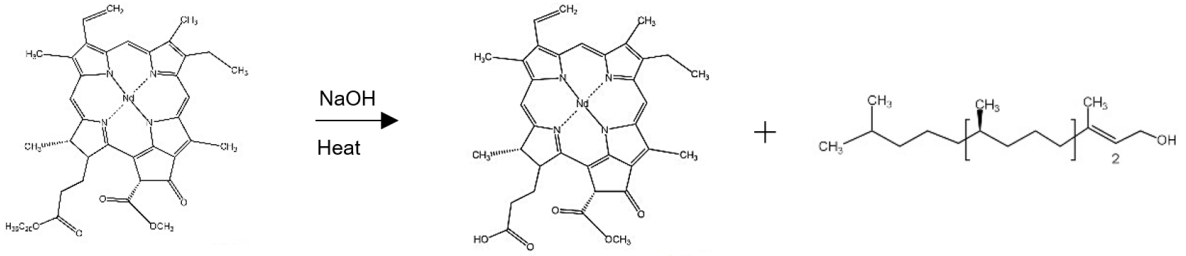

Figure 12. Hydrolysis reaction of Nd-pheophytin into Nd-pheophorbide.

The resulting Nd-pheophorbide complex has potential as a photodynamic therapy (PDT) agent. Complexation with Nd^{3+} ions can stabilize the pheophorbide structure and broaden the absorption spectrum, thereby enabling deeper light penetration into tissues. In addition, the Nd-pheophorbide complex also shows potential in theranostic systems. According to Jin et al. (2022), porphyrin–lanthanide complexes can enhance stability, improve cellular targeting, and efficiently produce singlet oxygen for cancer cell eradication.

Conclusion

Findings from the study reveal that 24-hour room-temperature and 10-hour reflux treatments produced distinct outcomes in the formation of the Nd-pheophytin complex. Nd-pheophytin synthesized at room temperature shows better results in the TLC analysis. UV-Vis spectrophotometry analysis showed a blue shift upon formation of Nd-pheophytin. The same pattern is also observed in emission spectra for Nd-pheophytin. Furthermore, TLC analysis of the hydrolysis product demonstrated a change in the Rf value from 0.90 to 0.45, confirming the formation of the more polar Nd-pheophorbide complex.

 E-ISSN: 2303-0720

Reference

Adhamatika, A., & Murtini, S. E. (2021). Pengaruh Metode Pengeringan Dan Persentase Teh Kering Terhadap Karakteristik Seduhan Teh Daun Bidara (Ziziphus mauritiana L.). *Jurnal Pangan Dan Agroindustri*, *9*(4), 196–207. https://doi.org/https://doi.org/10.21776/ub.jpa.2021.009.04.1

Adhitiyawarman, & Lowe, M. P. (2018). A New Zinc(II) Responsive MRI Contrast Agent. *Research Journal of Chemistry and Environment*, *22*(Special Issue II), 22–30.

Anjelia, R., Silalahi, I. H., & Gusrizal. (2019). Sintesis Dan Transisi Elektronik Senyawa Kompleks Klorofil Dengan Logam (M = Co2+, Fe3+). *Indonesian Journal of Pure and Appled Chemistry*, *2*(3), 102–111. https://doi.org/https://doi.org/10.26418/indonesian.v2i3.36891

Choi, C.-S. (2019). *The Design of Photobiological Active Molecular Model For Photodynamic Therapy*.

Das, D., Patil, S., & Gajbhiye, A. (2022). Heme-Mimetic Potential of Iron Conjugated Pheophytin-I in Attenuating Oxidative Stress-Induced Cellular and Vascular Toxicity. *Journal of Pharmacy and Bioallied Sciences*, *14*(Suppl 1), S115–S122. https://doi.org/10.4103/jpbs.jpbs_654_21

Erzunov, D. A., Bontar, A. A., Futerman, N. A., Vashurin, A. S., & Pukhovskaya, S. G. (2022). A simple Way To Obtain Stable Mono-decker Porphyrin Complexes With Heavy Metal Atoms. *Inorganic and Nano-Metal Chemistry*, *52*(2), 181–184. https://doi.org/10.1080/24701556.2021.1884712

Jin, G.-Q., Chau, C. V., Arambula, J. F., Gao, S., Sessler, J. L., & Zhang, J.-L. (2022). Lanthanide Porphyrinoids as Molecular Theranostics. *Chemical Society Reviews*, *51*(14), 6177–6209. https://doi.org/10.1039/D2CS00275B

Kang, Y. R., Park, J., Jung, S. K., & Chang, Y. H. (2018). Synthesis, characterization, and functional properties of chlorophylls, pheophytins, and Zn-pheophytins. *Food Chemistry*, *245*, 943–950. https://doi.org/10.1016/j.foodchem.2017.11.079

Kusmita, L., Puspitaningrum, I., & Limantara, L. (2015). Identification, Isolation and Antioxidant Activity of Pheophytin from Green Tea (Camellia Sinensis (L.) Kuntze). *Procedia Chemistry*, *14*, 232–238. https://doi.org/10.1016/j.proche.2015.03.033

Lopes, C. R. B., & Courrol, L. C. (2023). Evaluation of Steady-State and Time-Resolved Fluorescence Spectroscopy as a Method for Assessing the Impact of Photo-Oxidation on Refined Soybean Oils. *Foods*, *12*(9). https://doi.org/10.3390/foods12091862

Majid, T. S., & Muchtaridi, M. (2018). Aktivitas Farmakologi Ekstrak Daun Katuk (*Sauropus androgynus* (L.) Merr). *Farmaka*, *16*(2), 398–405.

Mohammed, H. A., Al-Omar, M. S., El-Readi, M. Z., Alhowail, A. H., Aldubayan, M. A., & Abdellatif, A. A. H. (2019). Formulation of Ethyl cellulose Microparticles Incorporated Pheophytin a Isolated From Suaeda Vermiculata for Antioxidant and Cytotoxic Activities. *Molecules*, *24*(8). https://doi.org/https://doi.org/10.3390/molecules24081501

Nandiyanto, A. B. D., Oktiani, R., & Ragadhita, R. (2019). How To Read and Interpret FTIR Spectroscope of Organic Material. *Indonesian Journal of Science and Technology*, *4*(1), 97–118. https://doi.org/10.17509/ijost.v4i1.15806

Notonegoro, H., Djamaludin, H., Setyaningsih, I., & Tarman, K. (2022). Fraksinasi Flavonoid Spirulina platensis dengan Metode Kromatografi Lapis Tipis dan Aktivitas Inhibisi Enzim α-Glukosidase. *Jurnal Kelautan Tropis*, *25*(3), 299–308. https://doi.org/10.14710/jkt.v25i3.13905

Nurdin, Kushart, C. M., Tanziha, I., & Januwat, M. (2009). Kandungan Klorofil Berbagai Jenis Daun Tanaman Dan Cu-Turunan Klorofil Serta Karakteristik Fisiko-Kimianya. *Jurnal Gizi Dan Pangan*, *4*(1), 13–19. https://doi.org/https://doi.org/10.25182/jgp.2009.4.1.13-19

Orzeł, Waś, J., Kania, A., Susz, A., Rutkowska-Zbik, D., Staroń, J., Witko, M., Stochel, G., & Fiedor, L. (2017). Factors Controlling The Reactivity of Divalent Metal Ions Towards Pheophytin a. *Journal of Biological Inorganic Chemistry*, *22*(6), 941–952. https://doi.org/10.1007/s00775-017-1472-1

Pasaribu, M. N., Pramesti, R., & Sedjati, S. (2025). Pembentukan Zona Hambat Patogen Staphylococcus aureus dan Escherichia coli terhadap Pigmen Fukosantin Ekstrak Sargassum polycystum C. Agardh. *Journal of Marine Research*, *14*(1), 72–78. https://doi.org/10.14710/jmr.v14i1.47898

 E-ISSN: 2303-0720

Pesang, M. D., Ngginak, J., Kase, A. G. O., & Bisilissin, C. L. B. (2020). Komposisi Pigmen pada Ulva sp., Padina australis dan Hypnea sp. dari Pantai Tablolong Provinsi Nusa Tenggara Timur. *Jurnal Kelautan Tropis*, *23*(2), 225–233. https://doi.org/10.14710/jkt.v23i2.5912

Pratiwi, R., Wahyuni, N., Hairil Alimuddin, A., & Hadari Nawawi, J. H. (2015). Uji Fotostabilitas TiO2-Klorofil Dari Mikroalga (Chlorella sp.). *Jurnal Kimia Khatulistiwa*, *4*(3), 59–64.

Quach, H. T., Steeper, R. L., & William Griffin, G. (2004). An Improved Method for the Extraction and Thin-Layer Chromatography of Chlorophyll a and b from Spinach. *Journal of Chemical Education*, *81*(3), 385–387. https://doi.org/https://doi.org/10.1021/ED081P385

Resita, D., Merdekawati, Susanto, AB., & Limantara, L. (2010). Kandungan dan Komposisi Pigmen Sargassum sp. pada Perairan Teluk Awur, Jepara dengan Perlakuan Segar dan Kering. *Jurnal Perikanan (Journal of Fisheries Sciences)*, *XII*(1), 11–19. https://www.researchgate.net/publication/337621101

Riansyah, H., Maulidya Maharani, D., Nugroho, A., Teknologi Industri Pertanian, J., Pertanian, F., Lambung Mangkurat Jalan Yani Km, U. A., & Selatan, K. (2021). Intensitas Dan Stabilitas Warna Ekstrak Daun Pandan, Suji, Katuk, Dan Kelor Sebagai Sumber Pewarna Hijau Alami. *Nal Riset Teknologi Industri*, *15*(1), 103–112. https://doi.org/https://doi.org/10.26578/jrti.v15i1.6549

Saide, A., Lauritano, C., & Ianora, A. (2020). Pheophorbide A: State of the art. *Marine Drugs*, *18*(5), 257. https://doi.org/10.3390/md18050257

Saleh, I., & Halidun, W. O. N. S. (2022). Identifikasi Pigmen Klorofil Dan Celah Energi Pada Daun Cincau (Cyclea Barbata) Sebagai Fotosensitizer Alami Untuk Aplikasi DSSC. *Jurnal Kumparan Fisika*, *5*(1), 31–36. https://doi.org/10.33369/jkf.5.1.31-36

Sandiningtyas, R. D., & Suendo, V. (2010). Isolation of Chlorophyll a From Spinach and Its Modification Using Fe2+ In Photostability Study. *The International Conference on Mathematics and Natural Sciences*. https://www.researchgate.net/publication/265490978

Sekali, E. E. K., Wartini, N. M., & Suhendra, L. (2020). Karakteristik Ekstrak Aseton Pewarna Alami Daun Singkong (Manihot Esculenta C.) pada Perlakuan Ukuran Partikel Bahan dan Lama Maserasi. *Jurnal Ilmiah Teknologi Pertanian Agrotechno*, *5*(2), 49–58. https://doi.org/https://doi.org/10.24843/jitpa.2020.v05.i02.p02

Sumiati. (2021). Penggunaan Pelarut Etanol dan Aseton pada Prosedur Kerja Ekstraksi Total Klorofil Daun Jati (Tectona grandis) dengan Metode Spektrofotometri. *Indonesian Journal of Laboratory*, *4*(1), 30–35. https://doi.org/https://doi.org/10.22146/ijl.v4i1.65418

Suria, Y., Ali, N. F. M., & Masrida, W. ode. (2024). Karakterisasi Senyawa Antibakteri Dari Ekstrak Biji Labu Kuning (Cucurbita Moschata Duch). *Jurnal Penelitian Sains Dan Kesehatan Avicenna*, *3*(3), 214–226. https://doi.org/https://doi.org/10.69677/avicenna.v3i3.106

Syahadat, A., Siregar, N., Studi, P., Program, F., Fakultas, S., Universitas, K., Royhan, A., & Kotapadangsidimpuan, D. (2020). Skrining Fitokimia Daun Katuk (*Sauropus androgynus*) Sebagai Pelancar ASI. *Jurnal Kesehatan Ilmiah Indonesia*, *5*(1), 85–89. https://doi.org/https://doi.org/10.51933/health.v5i1.246

Syahputri, Y., Sutanto, Mahmudin, M. D., & Ramadhan, M. R. I. (2024). Detection of Pb(II) and Cr(III) Using Dy(III) Ion with Pyrazoline Derivatives Ligand. *Jurnal Sains Natural*, *14*, 135–141. https://doi.org/https://doi.org/10.31938/jsn.v14i3.733

Tao, Y., Zhao, G., Yang, J., Ikeda, S., Jiang, J., Hu, T., Chen, W., Wei, Z., & Hong, F. (2001). Determination of double decker sandwich structured La-substituted chlorophyll a by EXAFS. *J. Synchrotron Radiat*, *8*, 996–997. https://doi.org/https://doi.org/10.1107/s0909049500019543

Usman, Fitri, I. A., & Suryani, C. L. (2022). Pengaruh Jenis Medium Sumber Zn2+ dan Lama Blanching Terhadap Aktivitas Antioksidan Bubuk Simplisia Sambiloto (Andrographis Paniculata). *Prosiding Seminar Nasional Mini Riset Mahasiswa*, *1*(2), 54–66.

Utami, W. W., & Anjani, G. (2016). Yogurt Daun Katuk Sebagai Salah Satu Alternatif Pangan Berbasis Laktogenik. *Journal of Nutrition College*, *5*(4), 513–519. https://doi.org/https://doi.org/10.14710/jnc.v5i4.16467

Wahyuni, I. T., & Setiarso, P. (2022). Karakterisasi Elektrokimia Ekstrak Klorofil dari Daun Salam (Syzgium polyanthum) pada pH Basa sebagai Sensitizer pada Dye Sensitized Solar Cell (DSSC). *Alchemy: Journal Of Chemistry*, *10*(2), 41–47. https://doi.org/https://doi.org/10.18860/al.v10i2.14109

 E-ISSN: 2303-0720

Wihenti, A. I., Supriyadi, & Santoso, U. (2021). Karakteristik Fisik dan Kimia Kelobot Jagung (Zea mays) Sebagai Bahan Pengemas. *Warta IHP*, *38*(1), 46–53. https://doi.org/https://doi.org/10.32765/wartaihp.v38i1.6416

Yusprianto, M., Zaharah, T. A., & Silalahi, I. H. (2021). Bandgap Energy of TiO_2/M-Chlorophyll Material (M=Cu^{2+}, Fe^{3+}). *Jurnal Kimia Sains Dan Aplikasi*, *24*(4), 126–135. https://doi.org/10.14710/jksa.24.4.126-135